

Numerical Simulation Study on Steel Pipe Row Pile Support of Temporary Road Slope

Jian-guang BAI , Hai-jun LI*

College of Energy and Transportation Engineering, Inner Mongolia Agricultural University, Hohhot 010018, China

Received 11 Jun 2022

Accepted 26 Oct 2022

Abstract

The slope stability analysis and support structure design of temporary roads are particularly important for the normal traffic of roads and the safe construction of underground structures. In this paper, FLAC^{3D} software is used to study the numerical simulation of steel pipe piles support structure of the slope of temporary road by using the equivalent stiffness method. It is shown that under the action of road load, the normal stress of steel pipe pile has a peak value at 1.0m above the bottom of foundation pit, and the shear stress has two peaks at 1.0m above the bottom of foundation pit and 0.5m above the pile tip, which decrease at the pile tip. The horizontal displacement of the pile occurs at different depth, the displacement of the pile top is the largest, and the displacement from the pile top to the bottom of foundation pit decreases nonlinearly, and the horizontal displacement of the pile below the bottom of foundation pit is very small and remains unchanged. The vertical displacement of the pile increases gradually from the pile top to the pile tip, which results in tensile deformation of the pile. Stress concentration occurs at the temporary road position in the slope, and obvious horizontal displacement and vertical displacement which have obvious differences in different positions appear in the slope. The arrangement of piles can ensure the stability of the slope and there will be no overall shear failure surface.

© 2022 Jordan Journal of Mechanical and Industrial Engineering. All rights reserved

Keywords: Temporary road; Steel pipe row pile; Slope support; FLAC^{3D} ; Numerical simulation.

1. Introduction

With the rapid development of social economy, urban population density increases sharply, and the demand for urban space is increasing while the utilization space is gradually shrinking. The space environment under urban roads becomes the main site for laying urban infrastructure such as water supply and drainage, telecommunications, power supply and heat supply. In order not to affect the normal operation of traffic, temporary roads should be built during the construction of underground works. The side of the temporary road close to the construction of underground works will form a slope due to the excavation of foundation pit, and its stability will directly affect the safety of the temporary road. Therefore, the slope stability analysis and slope support design of temporary roads are particularly important and become an important subject of geotechnical engineering.

Steel pipe row piles (hereinafter referred to as steel pipe piles) are mainly filled with concrete in seamless steel pipes. The surface between piles is woven with reinforcing mesh and sprayed with concrete to form an integral structure, which can not only ensure the stability of soil at the pile position, but also prevent the extrusion of soil between piles. Steel pipe piles have the characteristics of high strength and fast construction speed [1], and are widely used in engineering [2-5]. The construction site of underground works under urban roads is narrow and there

is not enough sloping space, so the temporary road on one side of the underground works will form a vertical slope. In view of the characteristics of steel pipe piles, steel pipe piles have become one of the preferred methods for slope support of temporary roads. Liu Aihuan etc. applied micro steel pipe piles in the protection of soft rock high slope and studied the stability of slope with steel pipe pile support structure [6]. Steel pipe piles are used for the expressway reconstruction project in soft soil areas, which can quickly construct and restore traffic in a short time. Therefore, steel pipe pile support structure has obvious advantages [7]. Slope protection pile and steel pipe pile are used to support the slope of deep foundation pit, which can ensure that the slope displacement is less than the safety alarm value given in the specification [8]. Park, No-Won etc. [9] studied the bending capacity of steel pipe piles through transverse pile load test and showed that steel pipe piles have higher bending capacity. Wang, XQ etc. [10] analyzed the influence of different cross-section parameters on the bending capacity of steel pipe piles. Moonkyung, Chung etc. [11] adopted 3D numerical simulation to analyze the yield behavior of pile material and the elastic-plastic behavior of soil, indicating that the horizontal bearing capacity of steel pipe pile is large.

Xiaoshuang Li, et al. used Midas GTS to simulate the three-dimensional static stability of the slope, and the slope's own frequency, damping characteristics, and dynamic response acceleration distribution after detonation were studied [12]. In order to reveal the deformation and

* Corresponding author e-mail: 326833988@qq.com.

failure process and evolution laws of fractured rock masses, semi-quantitative indicators such as the shape, quantity, density, size, distribution range, spatial position, and rock mass movement angle of the developed fissures were analyzed[13].Fadi Alfaqs used finite element method to study the fiber orientation effect on mid-plane transverse deflection and inter laminar shear stress[14].Louay S. Yousuf used ANSYS software to check and verify normal stresses[15].Benamar Balegh,et al.used finite element method to model the crevice corrosion effect on sheet pile steel,the results show that while a tensile strain enhances stress uniformly through sheet pile steel, an increasing depth of crevice corrosion results in a concentrated stress at localized corrosion[16].Therefore, numerical simulation is an effective method to study slope stability and structural mechanical properties [17].In this paper, FLAC^{3D} software is used to study the regularities of stress and deformation of steel pipe pile support structure and the effect of temporary road slope, so as to provide reference for rational use of steel pipe piles.

2. Introduction to FLAC^{3D} software

FLAC^{3D} is a 3D continuous fast Lagrange analysis software for numerical analysis of geotechnical engineering [18]. It adopts the mixed discrete element model [19] and the finite difference method to simulate the failure process of all kinds of rock and soil, so as to calculate the deformation and stress of rock and soil under various external loads. It has a relatively perfect post-processing function, and it is easy to realize data and results processing[20].It has been widely used in the fields of slope [21-24], stope[25, 26], roadway[27], foundation pit[28, 29] and tunnel[30, 31].

3. Modeling

3.1. Zones

In this paper, it is assumed that the soil under temporary road is homogeneous and isotropic, and the

Mohr-Coulomb model is adopted in the constitutive model.

The length of slope model is 30m in horizontal direction (X) , 5m in temporary road extension direction (Y) , and 18m in vertical direction(Z). Grid cells are divided every 1m in three directions. Eight-node hexahedron elements are adopted. The whole model includes 43,200 zones and 47,901 nodes. In the calculation of the model, the soil has been consolidated under the action of gravity.The acceleration of gravity is set at 10kN/m³, the temporary road load is strip and is set at 20kPa, and the range of action is one time of the depth of the foundation pit and 1.0m away from the top line of the foundation pit. Vertical excavation was carried out on one side of temporary road, and the excavation depth(D) was 6.0m. In order to facilitate pile modeling, the soil was divided into three groups of soil1, soil2 and soil3 through two planes X =27 and Z =6. The soil type and the parameters of each group are the same. The specific parameters were shown in Table 1, and the 3D entity model established is shown in Fig. 1.

Table 1. Basic parameters

Density (kg/m ³)	Cohesive force (kPa)	Internal friction angle (°)	Modulus of compression E_s (MPa)	Poisson's ratio μ
1860	16	24	6.8	0.25

The bulk modulus (K) and shear modulus (G) are calculated by equations (1) and (2) [32, 33] respectively, $K=13.6\text{MPa}$, $G=8.16\text{MPa}$.

$$K = \frac{E}{3(1-2\mu)} \quad (1)$$

$$G = \frac{E}{2(1+\mu)} \quad (2)$$

Where: E is the elastic modulus, $E= 3E_s$.

As the influence of temporary road load on the ground is mainly considered,the free constraint is adopted at $z=18$, lateral displacement constraint is adopted at the vertical side of the outer boundary $X=0$, $X=30$, $Y =0$ and $Y =5$, and fixed constraint condition is adopted at the bottom.

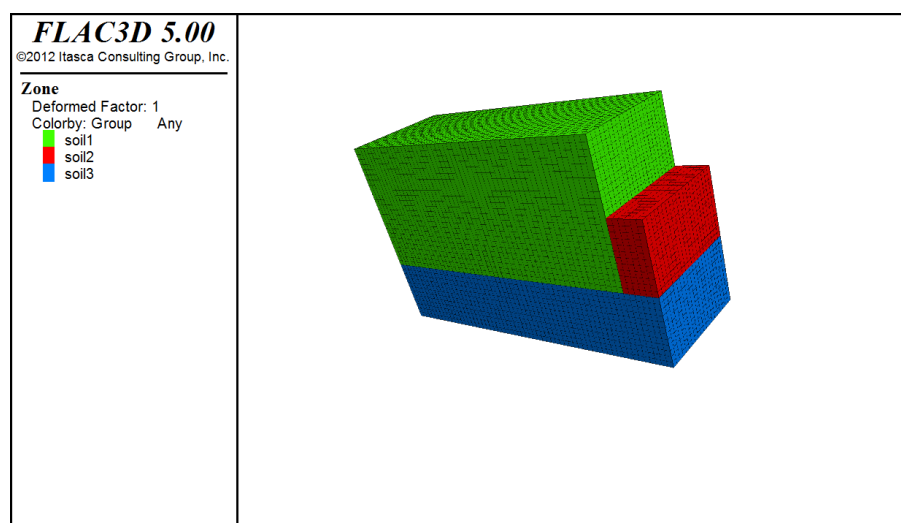


Figure 1. Zones model

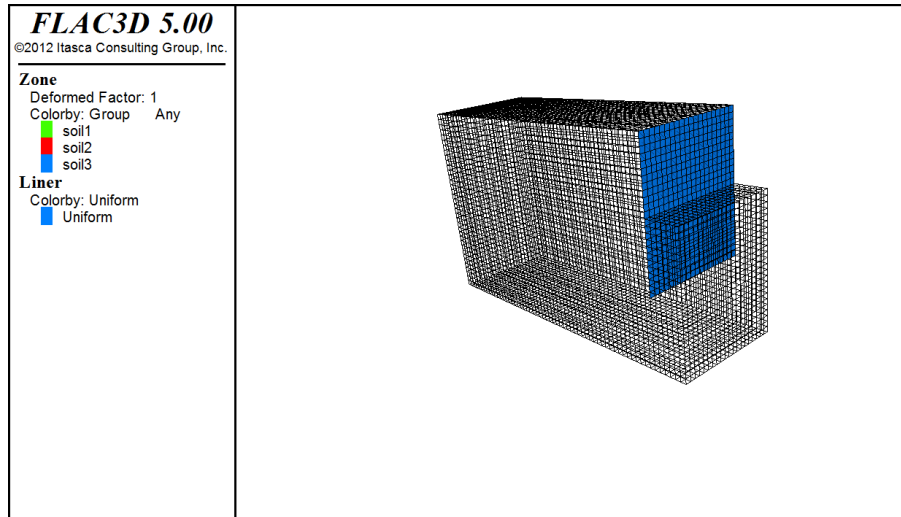


Figure 2. Structural element model

3.2. Structural elements

1. Element type

Steel mesh is laid between piles and concrete is sprayed on the surface of steel pipe pile support structure. The overall strength of support structure is provided by pile and concrete between piles. Liner element not only has certain bending resistance, but also can produce friction resistance with solid grid in shear direction. Taking the integrity of support structure and liner element attributes into consideration, liner structural element is used to simulate steel pipe piles, and discontinuous steel pipe piles are converted into continuous liner element. The established structural element model is shown in Fig.2. A total of 10 piles are arranged along the y axis direction, the pile length is 12m, the pile spacing is L=0.5m, the steel pipe material is seamless steel pipe, the yield strength is 235MPa, the type is 168mm×8mm, and the steel pipe is filled with C30 concrete. The equivalent stiffness method is adopted to convert the steel pipe piles into liner element and determine the liner element thickness, as shown in Fig. 3.

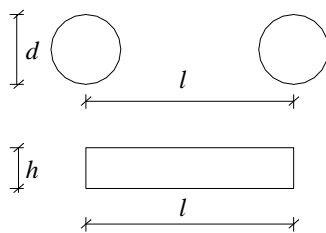


FIG.3 Diagram of equivalent stiffness

The steel pipe pile type is 168mm×8mm, the pile spacing is l=0.5m, so the moment of inertia $I_{x1} = \frac{\pi d^4}{64} = 3.098 \times 10^{-5} \text{ m}^4$. According to the equivalent stiffness method, the equivalent thickness of liner structural element is calculated according to equation 3, and the result is 0.098m.

$$I_{x1} = \frac{\pi d^4}{64} = I_{x2} = \frac{lh^3}{12} \tag{3}$$

2. Parameters Elastic modulus

The elastic modulus of steel pipe pile is calculated by weighted average of elastic modulus of steel pipe and concrete according to area. The elastic modulus of seamless steel pipe is 192GPa, and the elastic modulus of

C30 concrete is 30GPa, so the weighted elastic modulus of concrete-filled steel pipe pile is 59.39GPa.

3. Stiffness and strength

The stiffness kn and ks per unit area of normal and tangential coupling spring of the pile are taken as 10 times of the stiffness of the adjacent zones, and the normal surface stiffness of zones is calculated according to Formula (4). The result of kn and ks is $4.9 \times 10^5 \text{ KN/m}$. The tensile stiffness of pile-soil interface is 0, and the residual strength of pile-soil interface after failure is 0.

$$\max \left[\frac{K+4/3G}{\Delta z_{\min}} \right] \tag{4}$$

4. Other parameters

The cohesion between pile and soil is 0.8 times that of soil, so the cohesion is 12.8kPa and the internal friction angle is 19.2°. The density of steel pipe pile is 2500kg/m³.

4. Discussion

4.1. Numerical simulation analysis of steel pipe piles

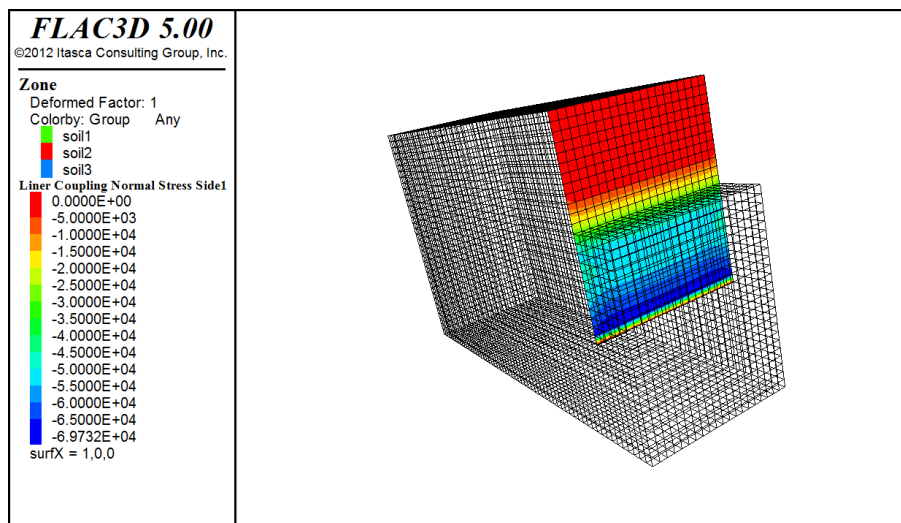
1. Stress of steel pipe piles

Figure 4(a) and Figure 4(b) respectively show the contour of normal stress and shear stress of steel pipe piles. As shown in Fig. 4(a), the normal stress of piles is zero between the pile top and 1.0m above the bottom of foundation pit. It increases first and then decreases from the position 1.0m above the bottom of foundation pit to the pile tip, and reaches its maximum at the position 0.5m above the pile tip. Pile tip effect occurs at the pile tip, and the normal stress decreases locally, which direction is the same as x negative direction. As shown in Fig. 4(b), the shear stress of piles has two peak values, which are located at 1.0m above the bottom of foundation pit and 0.5m above the pile tip. Pile tip effect occurs at the pile tip, and the normal stress decreases locally, which direction is the same as x negative direction. As shown in Fig. 4(b), the shear stress of piles has two peak values, which are located at 1.0m above the bottom of foundation pit and 0.5m above the pile tip. Pile tip effect occurs at the pile tip, and the normal stress decreases locally, which direction is the same as x negative direction. The shear stress on both sides of the first peak decreases gradually, and the range of action is from the pile top to the position half the depth below the bottom of foundation pit. The shear stress on both sides of the second peak decreases gradually, and the range of action is from the pile tip to the position half the depth below the bottom of foundation pit, which direction is the same as z negative direction.

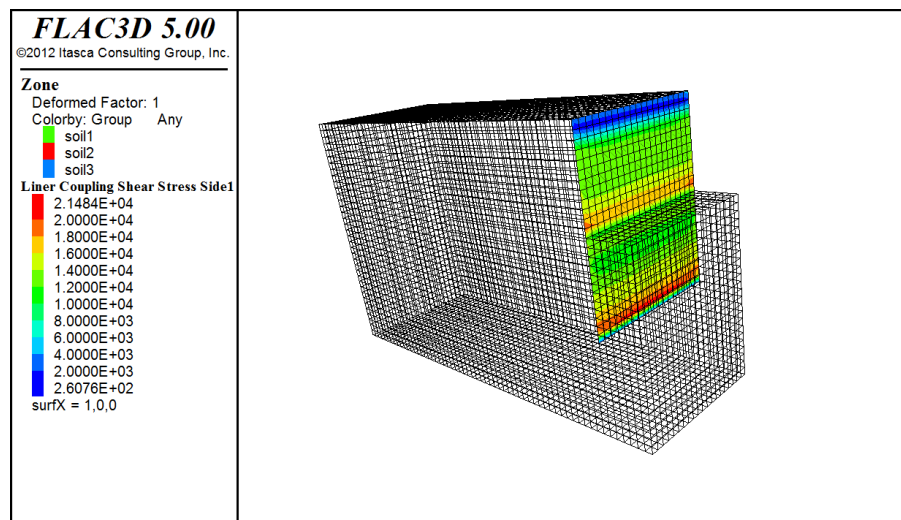
2. Displacement of steel pipe piles

The monitoring data show that the steel pipe pile will produce horizontal and vertical displacement under the action of earth pressure [35]. Figure 5(a) and Figure 5(b) respectively show the contour of Horizontal displacement and Vertical displacement of steel pipe piles. As shown in Fig. 5(a), different from the steel pipe pile with support [36], the cantilever steel pipe pile is subject to horizontal displacement under the action of earth pressure, and the displacement of the pile top is the largest [37], reaching 4.2cm. From the top of the pile to the bottom of the foundation, the displacement gradually decreases, and the reduction rate continuously decreases, showing a nonlinear decreasing trend in general, rather than increasing first and then decreasing [38]. The main reason is that the latter

adopts the combination of steel pipe pile and concrete row pile, which has strong stiffness and good bending resistance. From the bottom of the foundation pit to the pile tip, the displacement is consistent under the reverse extrusion of the soil under the bottom of the foundation pit, and the bending moment at the bottom of the foundation pit is the largest. As shown in Fig. 5(b), the steel pipe pile has vertical displacement. From pile top to pile tip, the displacement changes from 7.29mm to 7.35mm, and the relative displacement change rate of pile top is only 9.1%. The difference of vertical displacement between pile top and pile tip indicates that the pile has vertical tensile deformation.



(a)



(b)

Figure 4. Contour of stress of steel pipe piles
(a) Contour of Normal stress (b) Contour of Shear stress

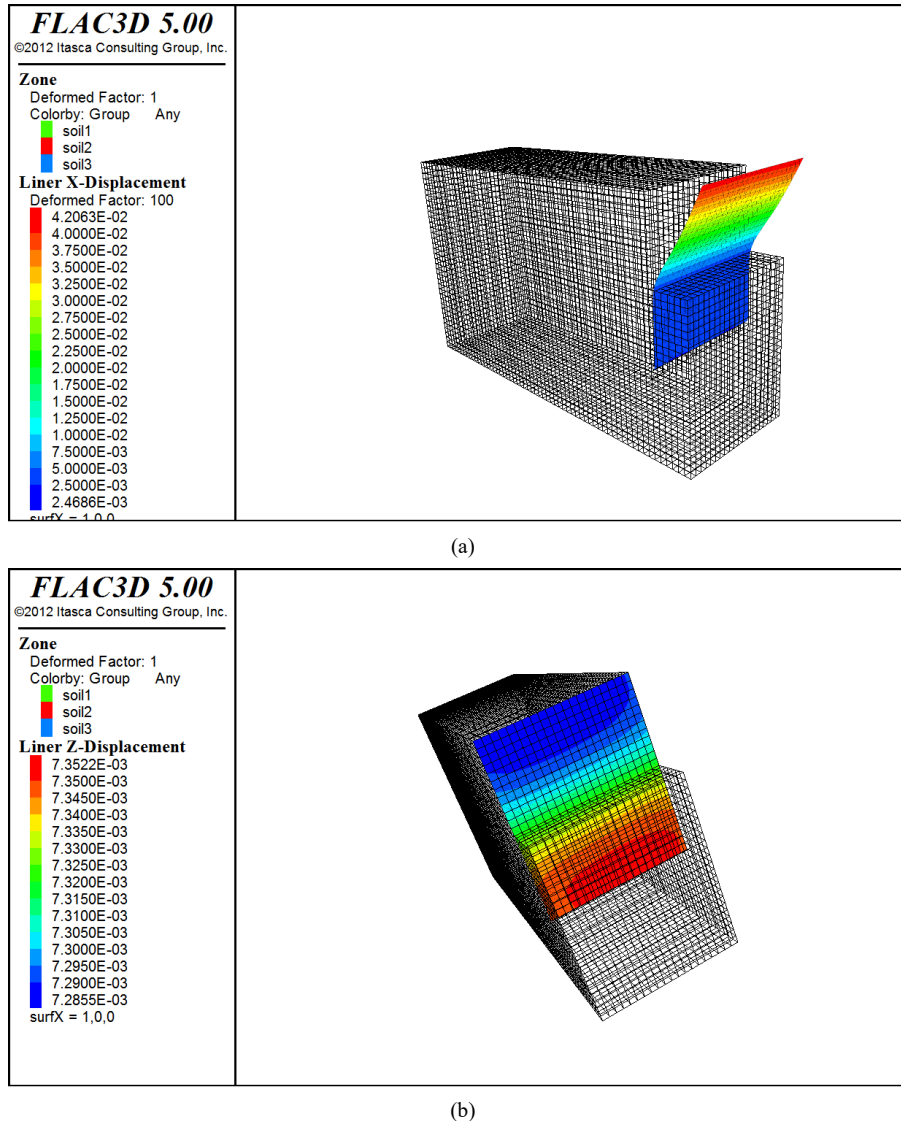


Figure 5. Contour of displacement of steel pipe piles
(a) Contour of Horizontal displacement (b) Contour of Vertical displacement

4.2. Numerical simulation analysis of slope

1. Displacement of slope

As shown in Fig. 6(a), the horizontal displacement of the slope increases first and then decreases from the position far away from the foundation pit to the position of the foundation pit. The displacement at the start point (0,5,18) is 0, and increases approximately linearly in the range of 0-15m. After 15m, the displacement increases gradually at a faster rate and reaches the maximum at 24.7m. Therefore, it is affected in the range of 4.5D away from the top line of the foundation pit, and begins to have a strong influence in the position of 2.0D (15m) away from the top line of the foundation pit. The displacement is the largest at the position 1/4 of the road width away from the road center towards the direction of the foundation pit. Limited by the piles, the displacement decreases towards the pile. The results indicate that centered on the position 1/4 of the road width away from the road center towards the direction of the foundation pit, the soil at the side far away from the center has a relative tensile effect, and the soil near the center has a relative compaction effect.

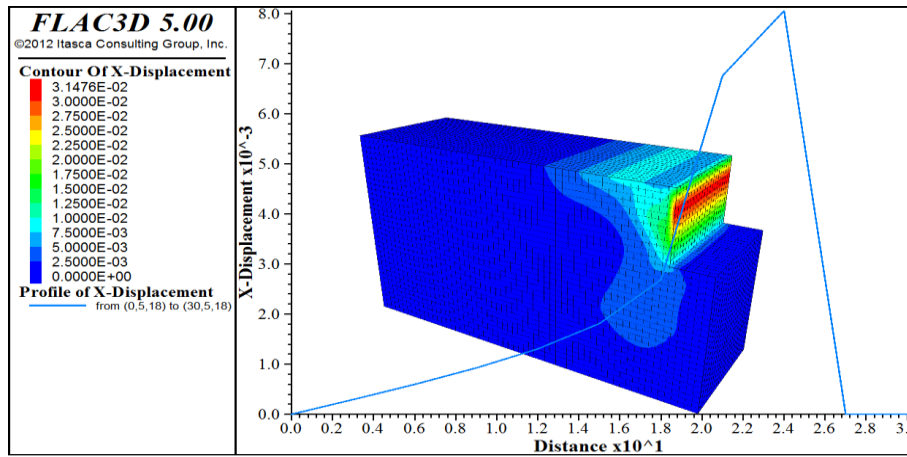
As shown in Fig. 6(b), affected by the temporary road load, the soil under the road has significant settlement, the displacement at the center of the road reaches 1.01cm. With the increase of the horizontal distance from the road, the vertical displacement of the slope on both sides of the road decreases gradually. Affected by the lateral limit of the pile, the vertical displacement near the piles increases, and the soil beside the pile rises upward. Along the depth direction, the vertical displacement is zero in the range of (1/3~2/3) D beside the pile above the bottom of foundation pit, and the displacement outside the range is positive. The soil beside the pile and at the bottom of the foundation pit rises upward. The vertical displacement of the slope away from the pile decreases gradually from the surface to the underground.

2. Slope sliding analysis

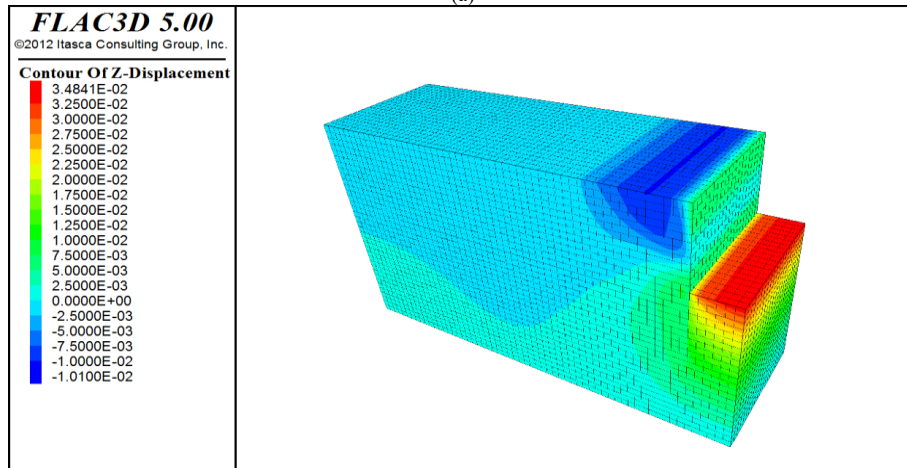
As shown in Fig. 7, the shear deformation mainly occurs in the soil at the pile position and the bottom of the foundation pit. In the 1/2D section downward from the ground surface, the shear deformation is mainly distributed between the top line of the foundation pit and the boundary line of the temporary road. From the surface downward, the

shear deformation tends to increase with the increase of depth, and the maximum shear deformation occurs in the range of $(1/4 \sim 1/2) d$ depth. In the section from $1/2D$ to the bottom of the foundation pit, the shear deformation decreases gradually from top to bottom, and it is not only distributed between the top line of the foundation pit and the boundary line of the temporary road, but also extends to the inside of the slope. The horizontal extension range is mainly distributed in the temporary road range, and does not extend to the surface. The shear strain increment gradually decreases from the piles to the inside, and no

through sliding surface is formed. In the section below the bottom of foundation pit, the shear deformation outside the pile row gradually decreases with the increase of the depth. The shear deformation of slope from the pile position along the horizontal direction to the inside of the foundation pit also decreases gradually, and it is the largest at the pile position at the bottom of the foundation pit. At the inner side of the piles, the shear deformation of the slope is obvious only at the depth of 1.5m below the bottom of the foundation pit, and the shear deformation below 1.5m is very small.



(a)



(b)

Figure 6. Contour of displacement of slope
(a) Contour of Horizontal displacement (b) Contour of Vertical displacement

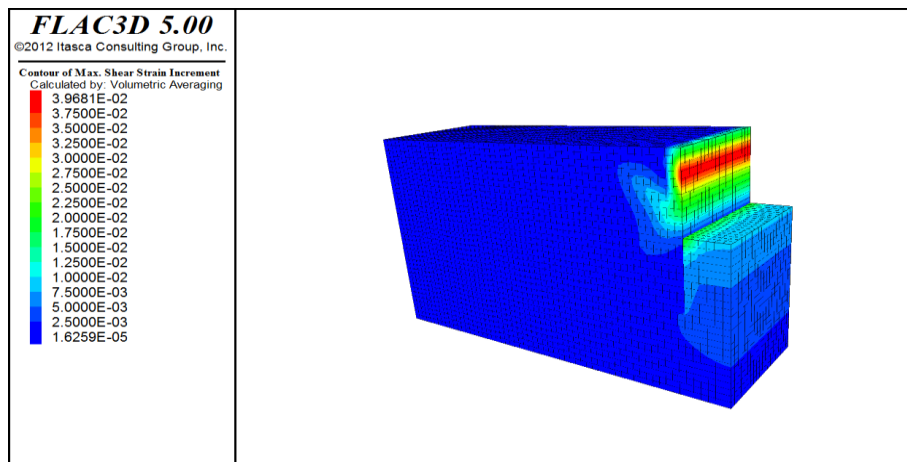


Figure 7. Contour of Max. shear strain increment

3. Slope stress analysis

Fig. 8 shows the contour slice of vertical stress determined with y as normal direction. According to the figure, the vertical stress in the slope gradually increases from the surface downward, and the stress is more concentrated at the position of temporary road. Therefore, the construction of temporary roads has an adverse impact on slope stability. At the same depth below the ground, the vertical stress of the pile position is lower than that of the ground without load. Therefore, the piles can not only bear the shear action in the horizontal direction, but also produce upward friction on the soil, which can reduce the vertical deformation of the soil. It indicates that the soil and pile have relative deformation. Below the bottom of the foundation pit, the stress changes on both sides of pile. The stress of soil in the excavation area increases locally in the range of 1/2 embedment depth, and decreases locally below the range of 1/2 embedment depth, and the stress of pile tip tends to be stable.

5. Validation analysis

Lizheng is the main software for the stability analysis of foundation pit slope, which is widely used in the actual slope support engineering design. The support design of the slope is calculated through Lizheng in the paper. The cohesion and internal friction angle of the soil layer used

in the calculation are shown in Table 1, some parameters are shown in Table 2, and the values of other parameters are the same as those used in the numerical simulation.

Table 2. Design parameters

Weight (kN/m ³)	Importance coefficient	Tensile, compressive and bending strength (MPa)	Shear strength (MPa)	Section plastic development coefficient
18.6	1.0	215	215	1.05

5.1. Stability analysis

The most unfavorable sliding surface is determined through the calculation of Lizheng. The Swedish slice method is adopted in the calculation, and the soil strip width of 1.0m is selected. The results show that the center coordinates of the most unfavorable sliding arc are (-1.947, 1.923) and the radius is 8.201 (as shown in Fig. 9). The integral stability safety coefficient of the slope is 2.490, greater than 1.30, meeting the specification requirements.

It can be seen from Fig. 7 that the slope with steel pipe pile support does not form a through sliding surface, the integral stability of the slope is good, and no sliding failure will occur. The numerical simulation is consistent with the calculation results of Lizheng design.

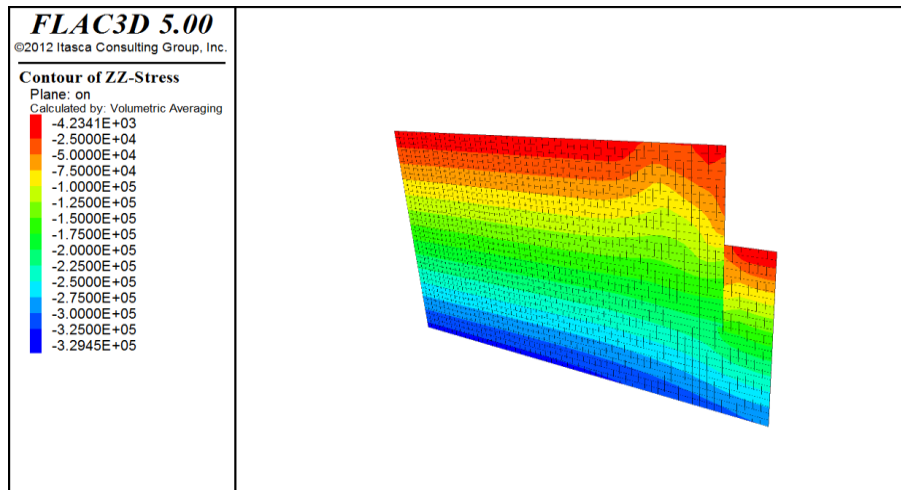


Figure 8. Contour slice of Vertical stress

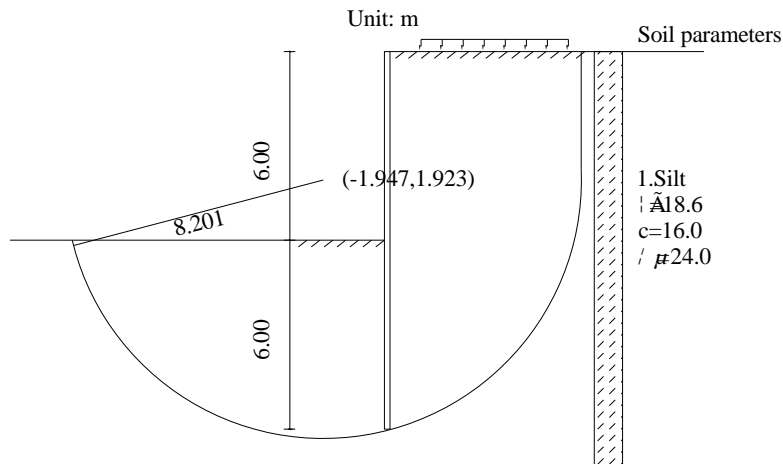


Figure 9. Integral stability (LiZheng software)

5.2. Displacement analysis

According to the comparison between Fig. 5 (b) and Fig. 6 (b), the vertical displacement of piles and soil at the same depth is different. It indicates that the piles and soil move relatively, resulting in friction on the contact surface. Because the vertical displacement of pile and soil is nonlinear, the friction is different at different depths. At the same depth, there is a difference in the horizontal displacement between the piles and the soil. The horizontal displacement of the row piles is greater than that of the soil, resulting in a certain degree of void between the piles and the soil, which is mainly caused by the bending deformation of the steel pipe piles due to the large bending moment near the bottom of the foundation [39]. The conclusion of slope stability shows that there is a certain degree of void between the piles and the slope, which will not affect the integral stability of the slope to a certain extent. Therefore, void phenomenon can be allowed to a certain extent in the actual design, which can save materials.

In the numerical simulation, the pile spacing is 500mm and the pile diameter is 168mm, so the distance diameter ratio is 2.98. As shown in Fig. 5 and Fig. 6, the maximum horizontal displacement of the slope is 3.1cm, and its maximum vertical displacement is 1.0cm. The maximum horizontal displacement of the pile is 4.2cm, and its maximum vertical displacement is 0.7cm. As the support structure is of class II, the monitoring alarm value specified in the specification is not exceeded [40]. Therefore, the arrangement of steel pipe piles with a distance diameter ratio of 2 [41] is not suitable for all situations. The reason is that the appropriate distance diameter ratio is related to the soil type of the slope, groundwater, ground load, crown beam setting and other factors, which need to be determined through comprehensive analysis.

As shown in Fig. 10, the maximum horizontal displacement of piles calculated by LiZheng is -466.39mm - -0.95mm, which is close to the maximum horizontal displacement of 420mm obtained by numerical simulation, and the error is only 9.9%, so the numerical simulation results are relatively reliable.

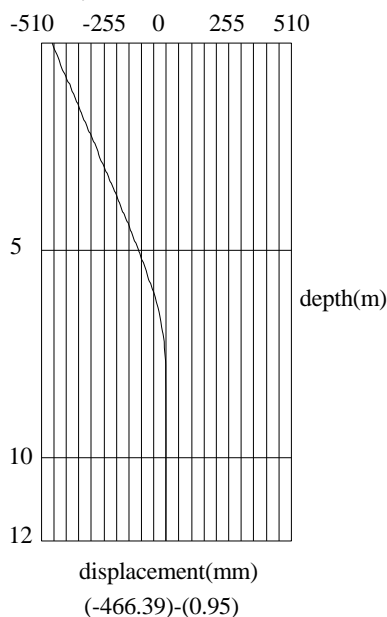


Figure 10. Displacement (LiZheng design)

6. Conclusions

1. The position 1.0m above the bottom of the foundation pit is the boundary point of pile stress. The normal stress increases from this point downward, and the shear stress peaks. The maximum normal stress occurs at 0.5m above the pile tip, and the shear stress peaks again. The normal stress and shear stress at pile tip decrease.
2. Due to the deformation of slope soil, the steel pipe pile has horizontal and vertical displacement under the action of soil. The bottom of the foundation pit is the boundary point of horizontal displacement. The horizontal displacement above the bottom of the foundation pit is large and changes obviously. The horizontal displacement at the pile top is the largest, and the displacement below the bottom of the foundation pit is very small. The vertical displacement of pile increases gradually from pile top to pile tip, and the relative displacement between pile and soil leads to friction, resulting in tensile deformation of pile.
3. The horizontal displacement of slope is the largest at the position 1/4 of the road width away from the road center towards the direction of the foundation pit. It gradually decreases to both sides, and the influence range mainly concentrates on the range of 4.5D away from the top line of the foundation pit. The vertical displacement of slope is the largest under the temporary road, and gradually decreases from the surface downwards. The vertical displacement near the pile increases upward and downward with $(1/3 \sim 2/3) D$ as the center. The influence of the vertical displacement in the horizontal direction exceeds the range of 4.5D from the excavation top line.
4. Small shear deformation occurs in the slope near pile, and the shear deformation is not obvious in the slope. It does not form a through sliding surface in the slope, and steel pipe piles can ensure the stability of the slope.
5. Affected by the load of the temporary road, the slope at the temporary road location produces stress concentration and causes displacement of the slope. The displacement of slope is different from that of pile, resulting in friction between slope and pile.

Expectation

Only a single type of soil is considered in the paper, the ground has no load other than that of the temporary road, and there is no groundwater. In practice, the stress and displacement of pile and slope are affected by a variety of factors, which should be comprehensively analyzed.

Void phenomenon between piles and the soil can be allowed to a certain extent in the actual design. Under the condition of ensuring the integral stability of the slope, the degree of voids allowed to occur needs to be further studied.

Acknowledgements

The authors would like to thank "the 13th five year plan" for educational science research in Inner Mongolia Autonomous Region (NGJGH2019402) for this study.

Reference

- [1]W. LI, K. Zhang, C.Y. Guo, Q. Cui, C.Q. Zhang, H.H. Ma, "Mechanical Properties and Microstructure an Pile-soil interface of Post-grouting Steel Pipe Pile". Science and Technology, Vol. 21, No. 19, 2021, 8159-8165.
- [2]M.Y. Zhang, J.X. Ma, S.J. Yang, Y.H. Wang, X.Y. Bai, S.X. Sun, "Experimental Study on Bending Moment of Double-Row Steel Pipe Piles in Foundation Excavation". Advances in Civil Engineering, 2020, 1-8.
- [3]H.W. Jin, "Design of Retaining and Protecting for a Deep Foundation Excavation". Advanced Construction Technologies, 2014, 1416-1420.
- [4]Y. Ishihama, J. Takemura, V. Kunasegaram, "Analytical evaluation of deformation behavior of cantilever type retaining wall using large diameter steel tubular piles into stiff ground". Geotechnics For Sustainable Infrastructure Development, No. 62, 2020, 91-98.
- [5]S.F. Zhang, C. Xia, H.C. Qin, T.F. Wang, Q.G. Chai, "Study on the Application of the Combined Retaining Structure of Anchor and Steel Pipe Pile in Reinforcement of High Fill Subgrade". Construction Technology(Chinese and English), Vol. 50, No. 19, 2021, 88-91+96.
- [6]A.H. Liu, Y.W. Zhao, K. Huang, H.L. Tang, "Application of Mini-Steel Pipe Piles in Soft Rock High Slope". Water Conservancy Science and Technology and Economy, Vol. 28, No. 04, 2022, 115-121.
- [7]J.L. Yan, "Application Analysis of Steel Pipe Pile Supporting Structure in Soft Soil Area". China Municipal Engineering, No. 01, 2022, 85-88+127.
- [8]J. Sun, M.H. Fan, X. Li, "Combined Supporting system of the Slope Protection Pile and the Compound Soil Nail Wall with Micro Steel Pipe Piles". Drilling Engineering, Vol. 48, No. 10, 2021, 116-124.
- [9]N.W. Park, K.H. Paik, "Lateral Behavior of Hybrid Composite Piles Using Prestressed Concrete Filled Steel Tube Piles". Journal of the Korean Geotechnical Society, Vol. 34, No. 12, 2018, 133-143.
- [10]X.Q. Wang, S.M. Zhang, Y.S. Huang, "Influences of Cross Section Parameters on Bending Resistance of TSC Pile". Advances in Civil and Industrial Engineering, 2014, 464-468.
- [11]C. Moonkyung, S.H. Lee, S.R. Kim, "Reinforcement Effect of Steel-Concrete Composite Group Piles by Numerical Analysis". Journal of the Korean Geotechnical Society, Vol. 26, No. 11, 2010, 29-38.
- [12]X. S. Li, Q. H. Li, Y. J. Hu, et al, "Study on Three Dimensional Dynamic Stability of Open-Pit High Slope under Blasting Vibration ". Lithosphere, Vol.2022,2022, 1-1731.
- [13]X. S. Li, Q. H. Li, Y. J. Hu, et al, " Evolution Characteristics of Mining Fissures in Overlying Strata of Stope after Converting from Open-Pit to Underground". Arabian Journal of Geosciences, Vol. 14, No.24, 2021, 1-18.
- [14]F.Alfaqs, " Dynamic Behavior of Thin Graphite/Epoxy FRP Simply Supported Beam Under Thermal Load Using 3-D Finite Element Modeling". Jordan Journal of Mechanical and Industrial Engineering, Vol. 15, No. 3, 2021, 301-308.
- [15]L.S. Yousuf, " The Effect of Temperature on the Stresses Analysis of Composites Laminate Plate". Jordan Journal of Mechanical and Industrial Engineering, Vol. 13, No. 4, 2019, 265-269.
- [16]B.Balegh, H. Trouzine, Y. Houmadi, "Finite Element Simulation and Prediction of Mechanical and Electrochemical Behavior on Crevice Corrosion in Sheet Pile Steel". Jordan Journal of Mechanical and Industrial Engineering, Vol. 12, No. 1, 2018, 23-31.
- [17]A.S. Alshyyab, F.H. Darwish, "Three-Dimensional Stress Analysis around Rivet Holes in a Plate Subjected to Biaxial Loading". Jordan Journal of Mechanical and Industrial Engineering, Vol. 12, No. 4, 2018, 323-330.
- [18]C. Sun, G.G. Yue, M.X. Li, "Study on the Influence of Pile Displacement of Foundation Pit Retaining Pile Based on Flac3D Numerical Simulation". Journal of Jilin Jianzhu University, Vol. 37, No. 02, 2020, 28-32.
- [19]Q.P. Xiao, Y.R. Zhong, X. Chen, X.L. Wang, "Analysis of Mechanical effect of Roadway Excavation and Support Based on Flac3D". Shandong Chemical Industry, Vol. 50, No. 22, 2021, 162-165+168.
- [20]J. Zhao, J.C. Sheng, B.Y. Su, Z.T. Zhang, "Method of Section -node Control for Mesh Auto-generation in 3D FEM Analysis". Journal of Yangtze River Scientific Research Institute, Vol. 17, No. 04, 2000, 34-37.
- [21]B. Hou, H.J. Jiang, "Stability Analysis of Maowu Slope Based on Flac3D Numerical Simulation Method". Jiangxi Building Materials, No. 07, 2021, 76-78.
- [22]H. Zhang, Z.G. Fan, "Treatment engineering and numerical simulation of a highway accumulation landslide based on FLAC3D". China Water Transport, Vol. 22, No. 02, 2022, 35-37.
- [23]Y. Tang, X. Yu, Z.H. Sun, "Study on Seismic Reinforcement Mechanism and Model of Anti-slide Piles based on FLAC3D". Hydropower Generation, Vol. 45, No. 07, 2019, 33-37.
- [24]Z.Y. Zou, H. Chen, Z.X. Wang, X.M. Long, L.Y. Chen, "Improvement of the strength reduction method on the basis of FLAC3D in slope stability". International Journal of Earth Sciences and Engineering, Vol. 9, No. 02, 2016, 486-491.
- [25]Q.H. Li, X.S. Li, J.B. Gen, L. Luo, "FLAC3D Numerical Simulation of Open-pit Transformation to Underground Slope and Stope Stability". Nonferrous Metals (mine part), Vol. 73, No. 02, 2021, 5-10.
- [26]Y.Q. Gong, G.L. Guo, "A data-intensive FLAC3D computation model: Application of geospatial big data to predict mining induced subsidence". Computer Modeling in Engineering and Sciences, Vol. 119, No. 02, 2019, 395-408.
- [27]J. Zhou, "Optimization Analysis of Wall Rock Support Parameters of Mining Roadway based on FLAC3D". China Mine Engineering, Vol. 50, No. 05, 2021, 49-52.
- [28]B. Qiu, "Impact of Foundation Pit Construction Process load on Surrounding Environment based on FLAC3D Simulation". Foundation & Structure Engineering, Vol. 37, No. 06, 2019, 245-247+251.
- [29]Y.F. Liu, S.G. Liu, "FLAC3D simulation analysis of excavation and supporting structure of deep foundation pit". International Journal of Earth Sciences and Engineering, Vol. 9, No. 05, 2016, 2321-2326.
- [30]S. Tang, J.X. He, X.L. Lin, "Study on the Pre-reinforcement Measures of Tunnel Shed with Soft Surrounding Rock based on FLAC3D". Subgrade Engineering, No. 05, 2021, 226-230.
- [31]Z.S. Shao, B.X. Li, "Study on Deformation and Secular Stability of Argillaceous Siltstoue Tunnel". Chinese Journal of Underground Space and Engineering, Vol. 17, No. 03, 2021, 883-896.
- [32]D.W. Song, F.M. Zhang, X.J. Han, Z.Q. Liu, "Analysis of the Deformation of the Soft and Hard Rock Interaction Slope based on FLAC3D". Journal of Hebei University of Engineering(Natural Science Edition), Vol. 33, No. 02, 2016, 86-90.
- [33]Q.Y. Meng, "Deformation and Stability Analysis of Excavated Slope by FEM". Journal of Hebei University of Engineering(Natural Science Edition), Vol. 27, No. 03, 2010, 32-34.
- [34]General Administration of Quality Supervision, Inspection and Quarantine of the People's Republic of China & Standardization Administration, Carbon Structural steels(GB/T700-2006). Peking: China Standards Press, 2006.

- [35]Y.W. Mao, J. Zhang, "Analysis on Monitoring the Supporting Effect of Micro Steel Pipe Pile Under the Condition of Miscellaneous Fill". *Urbanism and Architecture*, Vol. 17, No. 29, 2020, 113-114+117.
- [36]J. Rao, "Analysis on Application of Prefabricated Steel Pipe Pile Retaining Structure". *Urban Roads Bridges & Flood Control*, No. 11, 2021, 134-137+141+18.
- [37]B.Dong,Y.T. Zi,Y.W. Yang, "Miniature Steel Tube Pile Using in a Deep Foundation Pit in Coastal Area". *Shanxi Architecture*, Vol. 46, No. 13, 2020, 48-50.
- [38]J.Sun, "Combined Supporting System of the Slope Protection Pile and the Compound Soil Nail Wall with Micro Steel Pipe Piles". *Drilling Engineering*, Vol. 48, No. 10, 2021, 116-124.
- [39]F.G Hu, W.L. Chao, L.J. Feng, "Study on bearing failure mode of slope strengthened by micro single pile based on ultimate resistance". *Highway*, Vol. 65, No. 04, 2020, 12-18.
- [40]Construction Department of Shandong Province. *Technical Code for Monitoring of Building Excavation Engineering(GB50497-2009)*.Peking:China Planning Press;2009.
- [41]B.J. Yang,C.H. Zhu, "Numerical simulation of foundation pit based on steel pipe pile supporting system". *Water Conservancy Science and technology and Economy*, Vol. 26, No. 11, 2020, 65-69.